Supporting Information

Hterostructural MoS_2/NiS nanoflowers via precise interface modification for enhancing electrocatalytic hydrogen evolution

Xiwang Zhao[a], Jiehua Bao[a], Yuming Zhou[a*], Yiwei Zhang[a], Xiaoli Sheng[a], Bo Wu[b*], Yanyun Wang[a], Changjiang Zuo[a], Xiaohai Bu[c]

[a]Jiangsu Optoelectronic Functional Materials and Engineering Laboratory, School of Chemistry and Chemical Engineering, Southeast University, Nanjing 211189, P. R. China.

[b]Multiscale Computational Materials Facility, Key Laboratory of Eco-Materials Advanced Technology, College of Materials Science and Engineering, Fuzhou University, Fuzhou 350100, P. R. China.

[c] School of Materials Engineering, Nanjing Institute of Technology, Nanjing 211167, P. R. China

[*] Corresponding authors:

E-mail: ymzhou@seu.edu.cn (Y, Zhou)

wubo@fzu.edu.cn (B, Wu)

Tel./Fax: +86 25 52090617

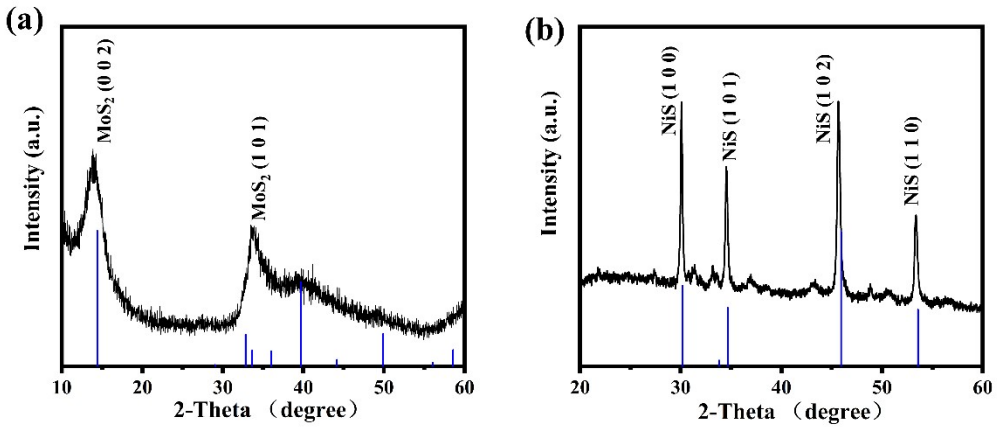

Figure S1 (a) The XRD patterns of pure MoS_2. (b) The XRD patterns of pure NiS nanostructures.

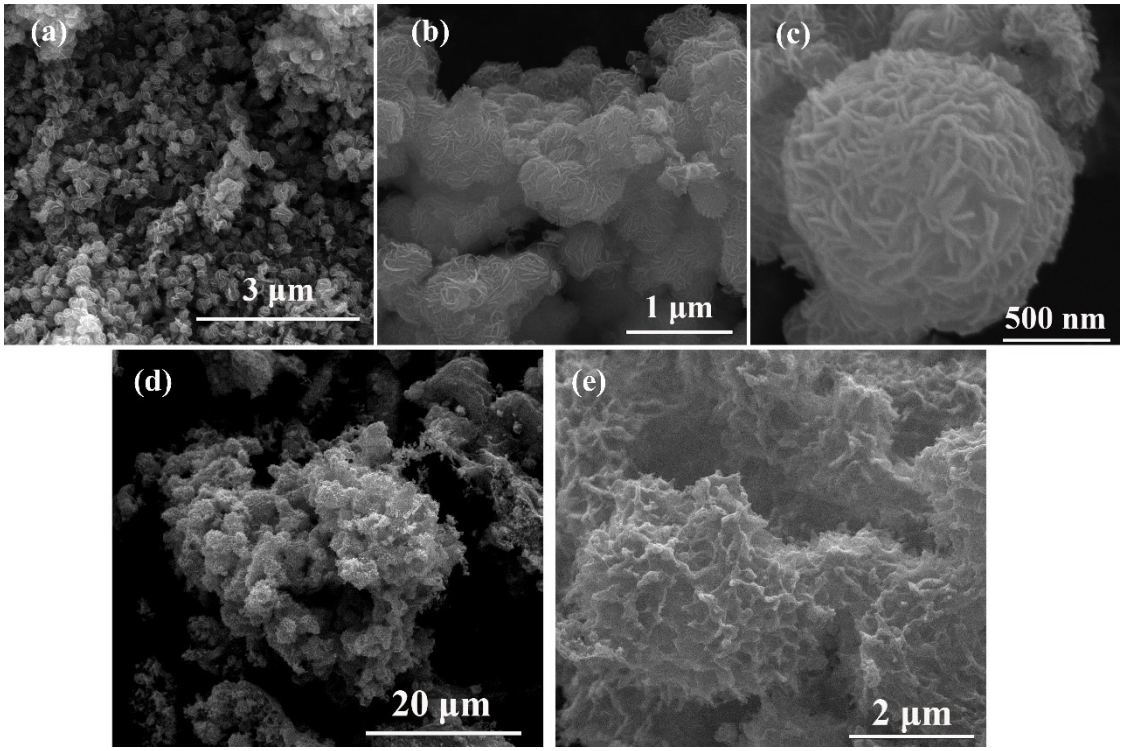

Figure S2 Different scale bar SEM images of the MoS_2 flowers like heterostructures (a) 3 µm, (b) 1 µm, (c) 500 nm. Different scale bar SEM images of the NiS nanostructures (d) 20 µm, (e) 2 µm.

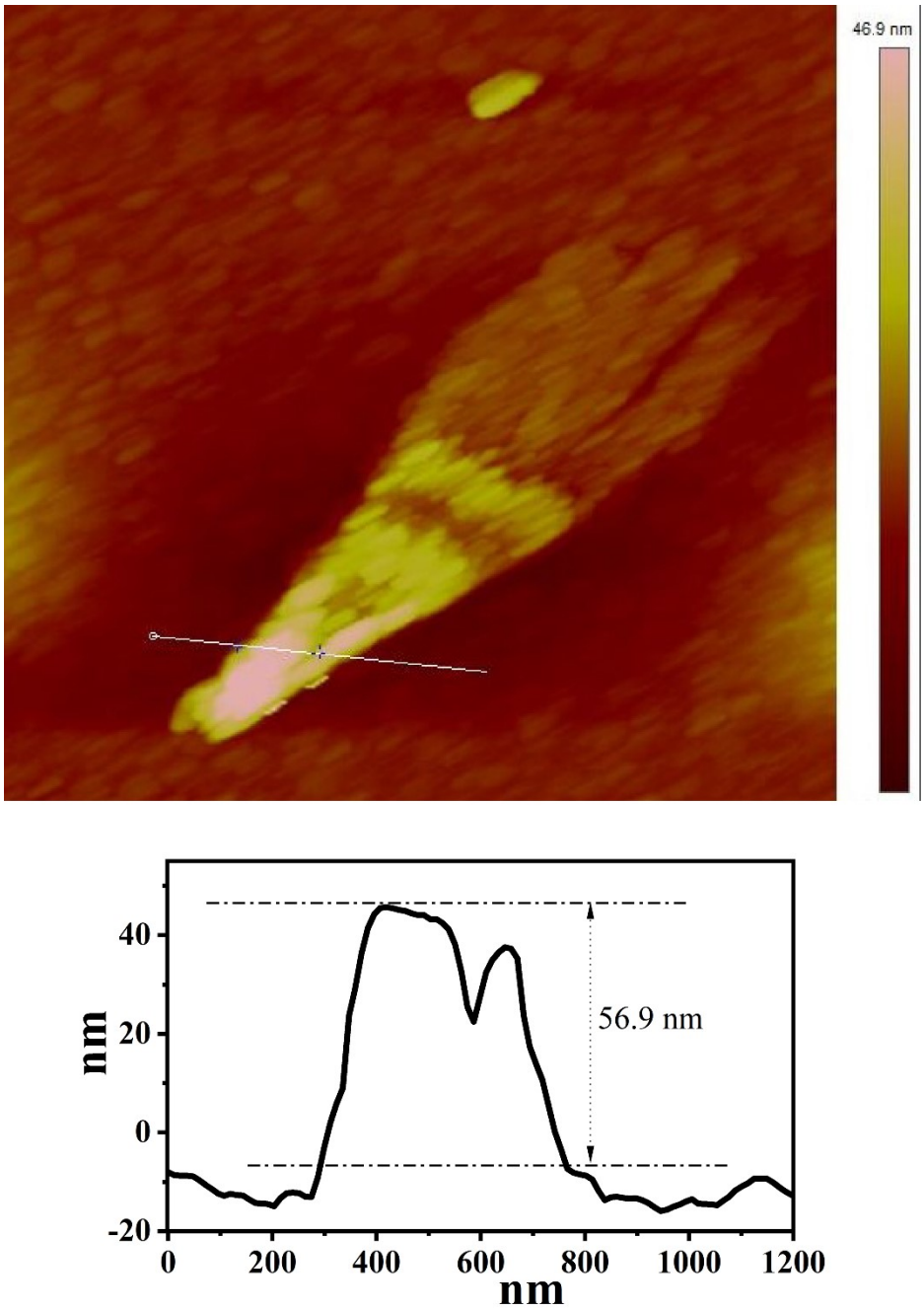

Figure S3 AFM image (top) and its height profile (bottom) along the white line of the MoS_2.

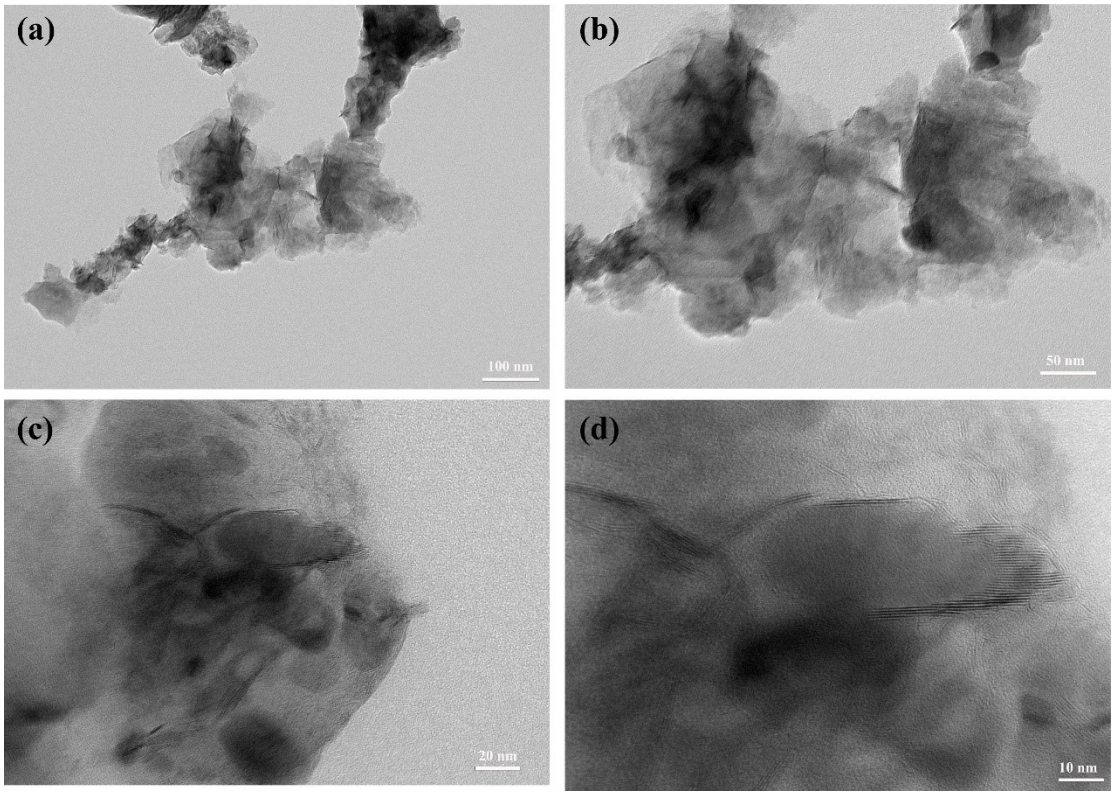

Figure S4 Different scale bar TEM images of the MoS_2/NiS flowers like heterostructures (a) 100 nm, (b) 50 nm, (c) 20 nm, (d) 10 nm.

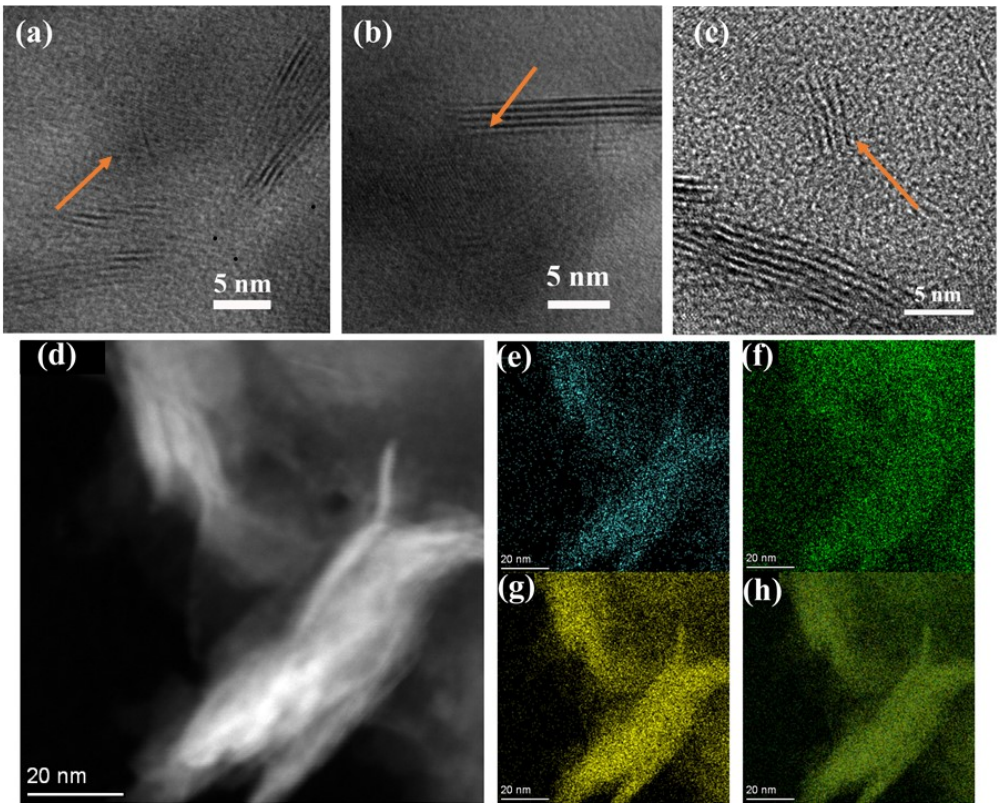

Figure S5 (a-c) The interface of the constructed MoS_2/NiS heterostructures. (d) The high-angle annular dark-field (HAADF) STEM image of MoS_2/NiS heterostructures and corresponding elemental mapping images of (e) Mo, (f) Ni, (g) S, and (h) overlap of the Mo, Ni, S.

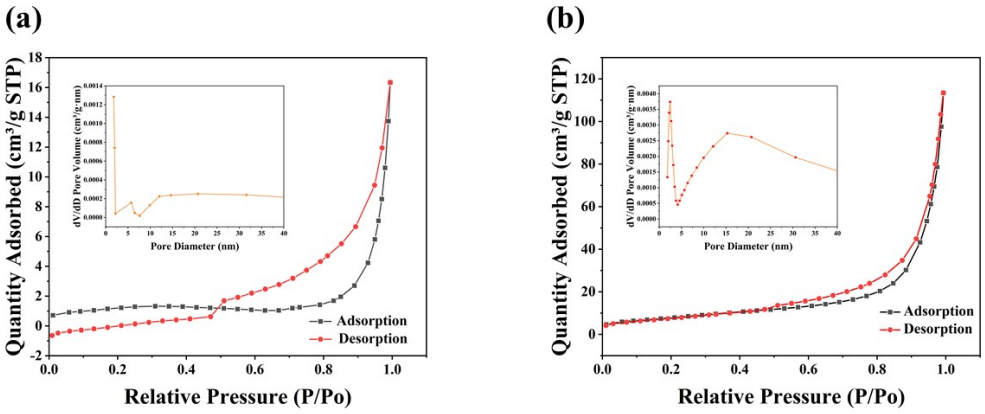

Figure S6 N_2 adsorption-desorption isotherm of (a) MoS_2, (b) MoS_2/NiS flowers like heterostructures, inset is the corresponding pore size distribution curve.

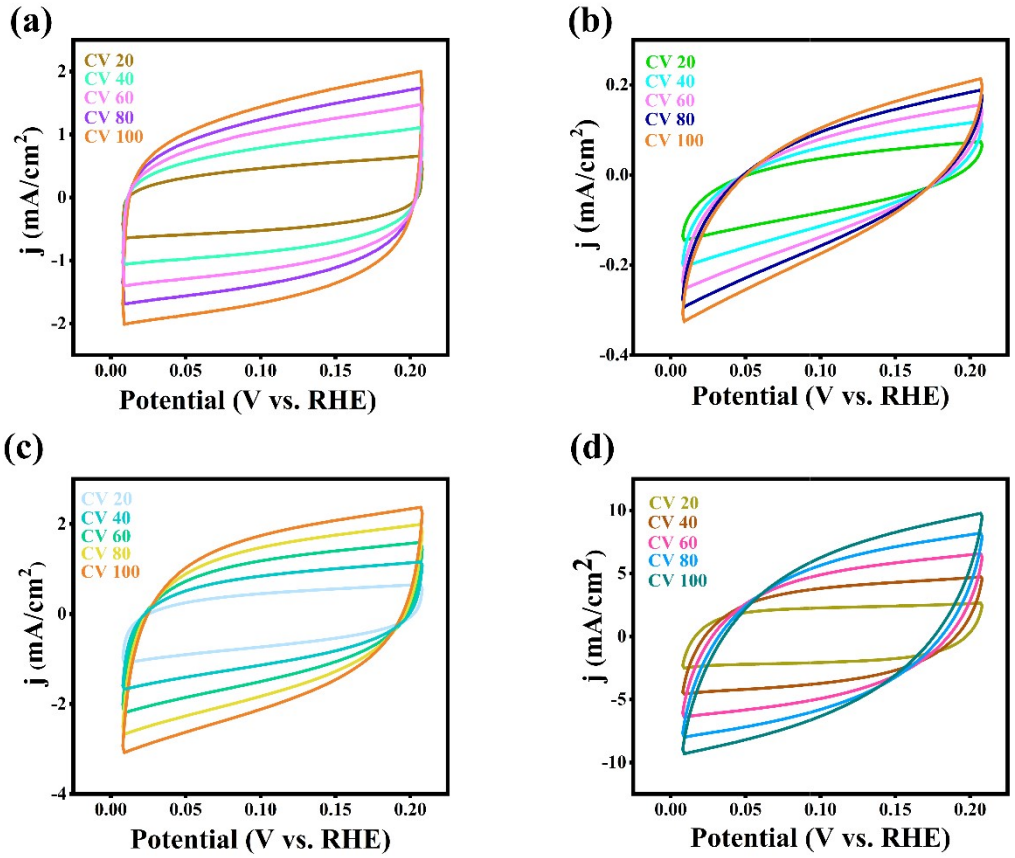

Figure S7 CV curves of (a) MoS_2, (b) NiS, (c) MoS_2/NiS flowers like heterostructures and (d) Pt/C.

At scan rates of 20, 40, 60, 80, 100 mV s^{-1} in 1.0 M KOH, respectively.

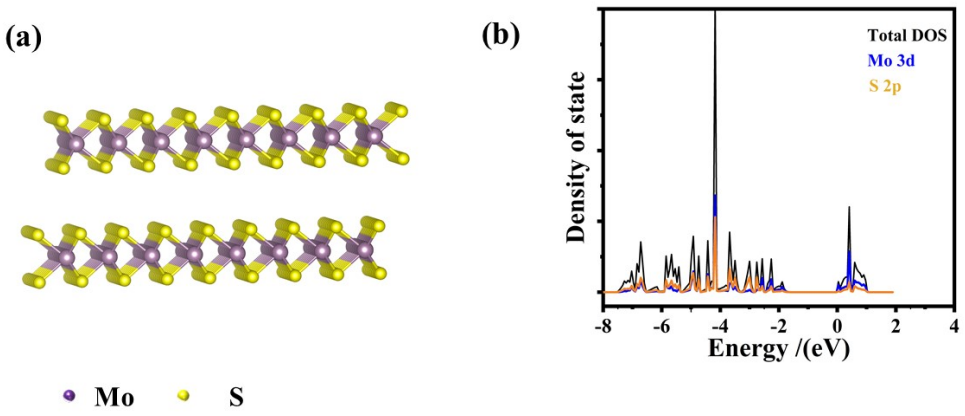

Figure S8 (a) MoS_2 (0 0 2) plane, (b) and the projected density of states of MoS_2 (0 0 2) plane.

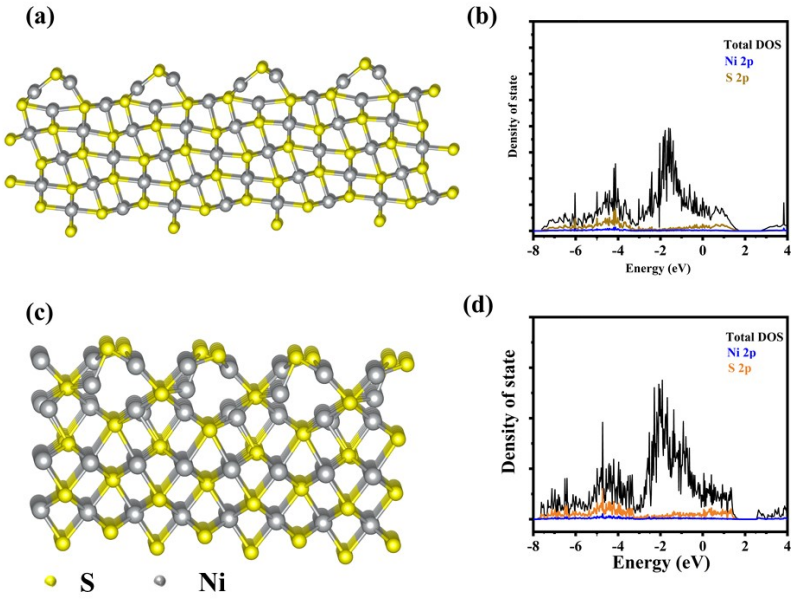

Figure S9 (a) NiS (1 0 2) plane, (b) and the projected density of states of NiS (1 0 2) plane, (c) NiS (1 0 0) plane, (d) and the projected density of states of NiS (1 0 0) plane.

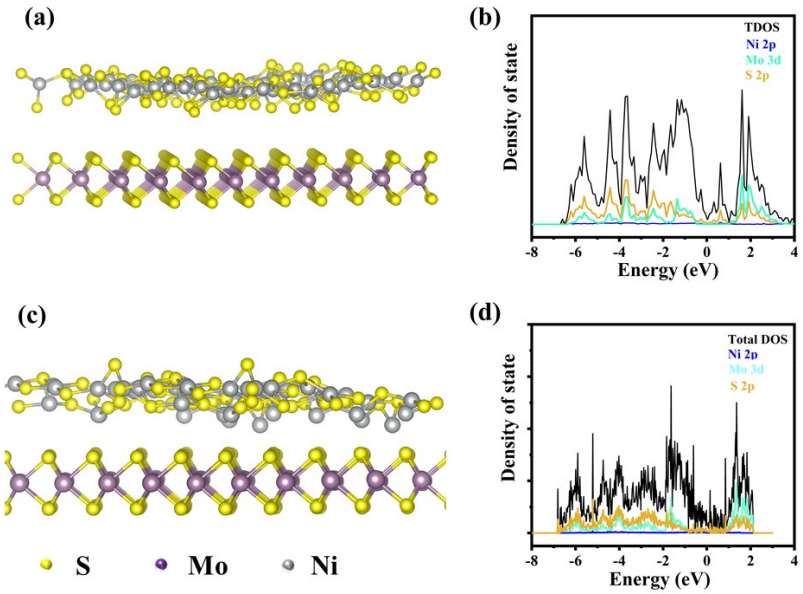

Figure S10 (a) Heterostructures constructed by using MoS_2 (0 0 2) crystal surface and NiS (1 0 0) crystal surface. (b) And the projected density of states of MoS_2/NiS heterostructures. (c) Heterostructures constructed by using MoS_2 (0 0 2) crystal surface and NiS (1 0 2) crystal surface, (d) and the projected density of states of MoS_2/NiS heterostructures.

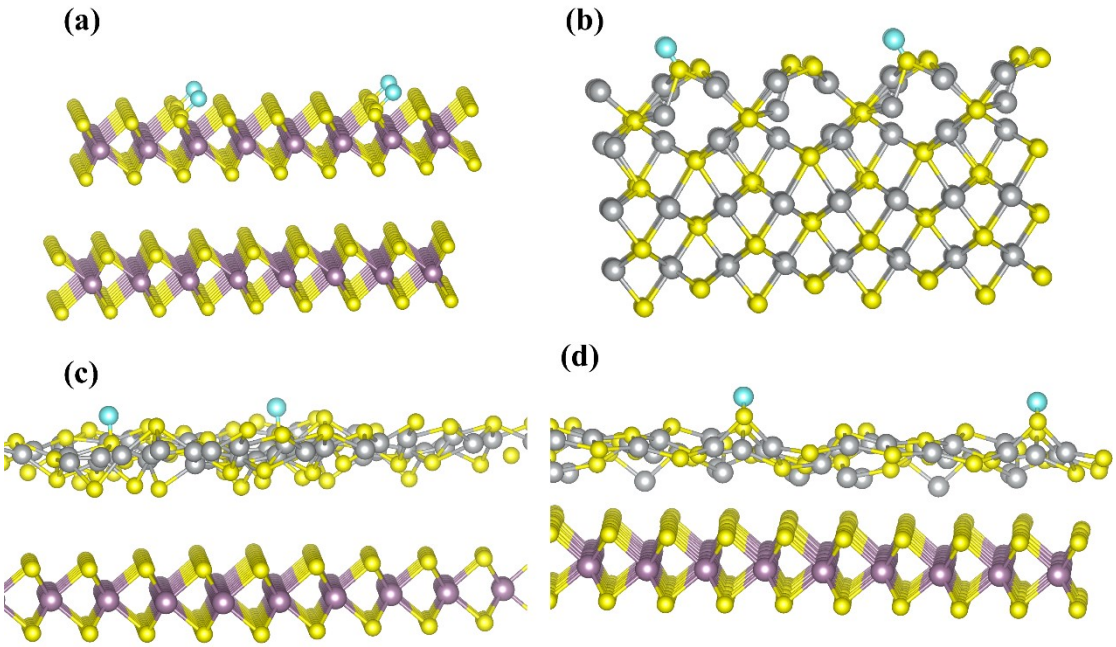

Figure S11 Hydrogen atoms adsorb on different DFT chemisorption models. (a) Hydrogen atoms adsorb on the MoS_2 (0 0 2) basal plane sites, (b) hydrogen atoms adsorb on the NiS (1 0 0) plane, (c) hydrogen atoms adsorb on the heterogeneous structure constructed by using MoS_2 (0 0 2) crystal surface and NiS (1 0 0) crystal surface, (d) hydrogen atoms adsorb on the heterogeneous structure constructed by using MoS_2 (0 0 2) crystal surface and NiS (1 0 2) crystal surface.

DFT models	**E_0 (eV)**	**ΔG (eV)**	**ΔG_{H^*} (eV)**
NiS (1 0 0) _slab	-633.777	0	
NiS (1 0 0) _H	-636.670	0.216	0.703
MoS_2 (0 0 2) _slab	-1395.438	0	
MoS_2 (0 0 2) _H	-1397.132	0.173	1.859
MoS_2 (1 0 0) _slab	-662.197	0	
MoS_2 (1 0 0) _H	-666.361	0.231	-0.553
MoS_2/NiS (1 0 0) _slab	-1032.172	0	
MoS_2/NiS (1 0 0) _H	-1035.277	0.220	0.525
MoS_2/NiS (1 0 2) _slab	-1062.910	0	
MoS_2/NiS (1 0 2) _H	-1066.030	0.222	0.482

Table S1 The specific values of the surface energy of differents slabs and the surface energy of hydrogen adsorption models.

Samples	η10 （mV）	Tafel （mV dec^{-1}）	Ref.
1T-2H Cr_x-MoS_2 Ultrathin Nanosheets	200	41.6	1
Al-MoS_2	198	134	2
VNMS	122	57	3
MoS_2 QDs/NiO NSs	186	73.5	4
Co-Ni-P/MoS_2	116	41	5
K-$G_{4.0}T_{2.0}Mo_{1.0}$	173	66.4	6
MoS_2/NiS-Ni_3S_2/NF	181	70	7
MoS_2/Ni_3S_2 foam	190	65.6	8
Cu_9S_5@MoS_2/CNFs	114	199	9
MoNiCNTs-4	238	84	10
Ni_2P/MoS_2	149	69.5	11
NCN-CoMoS-700	126	74.1	12
S-MoS_2@C	155	78	13
MoS_2/FNS/FeNi foam	122	45.1	14
Single-layer MoS_2	185	45	15
MoS_2/Ni_3S_2 heterostructures	110	83	16
MoS2/NiS heterostructures	**158**	**128.1**	**This work**

Table S2. Comparison of HER performance of electrocatalysts reported in different literatures in alkaline solution.

References

1. Jian, J.; Li, H.; Sun, X.; Kong, D.; Zhang, X.; Zhang, L.; Yuan, H.; Feng, S. *ACS Sustain. Chem. Eng.*, 2019, **7**, (7), 7227-7232.

2. Jian, J.; Li, Y.; Bi, H.; Wang, X.; Wu, X.; Qin, W. *ACS Sustain. Chem. Eng.*, 2020, **8**, (11), 4547-4554.

3. Bolar, S.; Shit, S.; Murmu, N. C.; Samanta, P.; Kuila, T. *ACS Appl. Mater. Inter.*, 2021, **13**, (1), 765-780.

4. Zhan, G.; Zhang, J.; Wang, Y.; Yu, C.; Wu, J.; Cui, J.; Shu, X.; Qin, Y.; Zheng, H.; Sun, J.; Yan, J.; Zhang, Y.; Tiwary, C. S.; Wu, Y. *J. Colloid Interf. Sci.*, 2020, **566**, 411-418.

5. Bao, J.; Zhou, Y.; Zhang, Y.; Sheng, X.; Wang, Y.; Liang, S.; Guo, C.; Yang, W.; Zhuang, T.; Hu, Y. *J. Mater. Chem. A*, 2020, **8**, (42), 22181-22190.

6. Zhang, W.; Yu, H.; Tang, D.; Huang, Y.; Wang, J.; Yang, L.; Zhao, Z. *Int. J. Hydrogen Energ.*, 2021, **46**, (27), 13936-13945.

7. Guan, Y.; Xuan, H.; Li, H.; Han, P. *Electrochim. Acta*, 2019, **320**, 134614.

8. Narasimman, R.; Waldiya, M.; K, J.; Vemuri, S. K.; Mukhopadhyay, I.; Ray, A. *Int. J. Hydrogen Energ.*, 2021, 2021, **46**, (11), 7759-7771.

9. Zhang, Z.; Zhu, H.; Hao, J.; Lu, S.; Duan, F.; Xu, F.; Du, M. *J. Colloid Interf. Sci.*, 2021, **595**, 88-97.

10. Zhang, X.; Yang, P.; Jiang, S. P. *Carbon*, 2021, **175**, 176-186.

11. Kim, M.; Anjum, M. A. R.; Lee, M.; Lee, B. J.; Lee, J. S. *Adv. Funct. Mater.*, 2019, **29**, (10), 1809151.

12. Kim, M.; Seok, H.; Clament Sagaya Selvam, N.; Cho, J.; Choi, G. H.; Nam, M. G.; Kang, S.; Kim, T.; Yoo, P. J. *J. Power Sources*, 2021, **493**, 229688.

13. Xu, Q.; Liu, Y.; Jiang, H.; Hu, Y.; Liu, H.; Li, C. *Adv. Energy. Mater.*, 2019, **9,** (2), 1802553 .

14. Wu, Y.; Li, F.; Chen, W.; Xiang, Q.; Ma, Y.; Zhu, H.; Tao, P.; Song, C.; Shang, W.; Deng, T.; Wu, J. *Adv. Mater.*, 2018, **30**, (38), 1803151.

15. Wan, Y.; Zhang, Z.; Xu, X.; Zhang, Z.; Li, P.; Fang, X.; Zhang, K.; Yuan, K.; Liu, K.; Ran, G.; Li, Y.; Ye, Y.; Dai, L. *Nano Energy*, 2018, **51**, 786-792.

16. Zhang, J.; Wang, T.; Pohl, D.; Rellinghaus, B.; Dong, R.; Liu, S.; Zhuang, X.; Feng, X. *Angew. Chem., Int. Ed.*, 2016, **55**, (23), 6702-6707.